Improvement in ionization efficiency of direct analysis in real time-mass spectrometry (DART-MS) by corona discharge

Kanako Sekimoto[1*], Motoshi Sakakura[2], Takatomo Kawamukai[2], Hiroshi Hike[2], Teruhisa Shiota[2], Fumihiko Usui[2], Yasuhiko Bando[2] and Mitsuo Takayama[1]

[1] Graduate School of Nanobioscience, Yokohama City University, 22-2 Seto, Kanazawa-ku, Yokohama, Kanagawa, 236-0027 Japan

[2] AMR Inc., 13-18 Nakane-2, Meguro-ku, Tokyo, 152-0031 Japan

Supporting Information

Table S1. Exact masses of the analyte-related ions observed in each mass spectrum shown in Figs. 6, 7, S2 and S3 and correponding accuracy.

Figure		Ion species	*m/z* Nominal mass	*m/z* Measured exact mass	*m/z* Calculated exact mass	Accuracy [ppm]
Figure 6 (Q Exactive™ Orbitrap™ MS)	a	$[Asn + H]^+$	133	133.0606	133.0608	-0.9300
	b	$[Trp + H]^+$	205	205.0969	205.0972	-1.0969
		$[Trp + H + O]^+$	221	221.0916	221.0921	-1.9955
		$[Trp + H + 2O]^+$	237	237.0870	237.0866	-1.7670
		$[Trp + H - NH_3]^+$	188	188.0704	188.0706	-1.0910
	c	$[Gly - H]^-$	74	74.0247	74.0248	1.0077
		$[Gly - 2H - H]^-$	72	72.0092	72.0091	1.1812
		$C_3H_5O_3^-$	89	89.0244	89.0244	-0.4739
	d	$[Tyr - H]^-$	180	180.0666	180.0666	0.1536
		$[Tyr - H + O]^-$	196	196.0615	196.0615	-0.1743
		$[Tyr - H - H_2CO_2]^-$	134	134.0612	134.0611	0.3006
		$[Tyr + C_3H_5O_3]^-$	270	270.0982	270.0983	-0.4745
		$C_3H_5O_3^-$	89	89.0244	89.0244	-0.4739
	e	$[Asn + H]^+$	133	133.0606	133.0608	-0.9300
	f	$[Trp + H]^+$	205	205.0969	205.0972	-1.0969
		$[Trp + H + O]^+$	221	221.0916	221.0921	-1.9955
		$[Trp + H + 2O]^+$	237	237.0870	237.0866	-1.7670
		$[Trp + H - NH_3]^+$	188	188.0704	188.0706	-1.0910
	g	$[Gly - H]^-$	74	74.0247	74.0248	1.0077
		$[Gly - 2H - H]^-$	72	72.0092	72.0091	1.1812
		$C_3H_5O_3^-$	89	89.0244	89.0244	-0.4739
	h	$[Tyr - H]^-$	180	180.0666	180.0666	0.1536
		$[Tyr - H + O]^-$	196	196.0615	196.0615	-0.1743
		$[Tyr - H - H_2CO_2]^-$	134	134.0612	134.0611	0.3006
		$[Tyr + C_3H_5O_3]^-$	270	270.0982	270.0983	-0.4745
		$C_3H_5O_3^-$	89	89.0244	89.0244	-0.4739
Figure 7 (Synapt G Q-TOF-MS)	a	$C_6H_{15}O_3^-$	135	135.1006	135.1021	-11.1
	b	$[PD + O - 3H]^+$	225	225.2251	225.2218	14.7
		$C_6H_{15}O_3^-$	135	135.1006	135.1021	-11.1
	c	$C_6H_{15}O_3^-$	135	135.1006	135.1021	-11.1
	d	$[TD + O - 3H]^+$	197	197.1924	197.1905	9.6
	e	$[PD + O - 3H]^+$	225	225.2251	225.2218	14.7
	f	$[HD + O - 3H]^+$	253	253.2570	253.2531	15.4
Figure S2 (Q Exactive™ orbitrap™ MS)	a	$[Gly + H]^+$	76	76.0392	76.0393	-0.8544
	b	$[Asp + H]^+$	134	134.0447	134.0448	-0.7952
		$[Asp + H - H_2O]^+$	116	116.0342	116.0342	-0.3971
	c	$[Tyr + H]^+$	182	182.0809	182.0812	-1.2122
		$[Tyr + H + O]^+$	198	198.0758	198.0761	-1.4860
		$[Tyr + H - H_2CO_2]^+$	136	136.0756	136.0757	-0.8819
	d	$[Ala + H]^+$	90	90.0549	90.0550	-0.9440
	e	$[Phe + H]^+$	166	166.0860	166.0863	-1.7571
		$[Phe + H - H_2CO_2]^+$	120	120.0805	120.0808	-1.9710
	f	$[Met + H]^+$	150	150.0580	150.0583	-2.3060
		$[Met + H + O]^+$	166	166.0530	166.0532	-1.3530
	g	$[Gly + H]^+$	76	76.0392	76.0393	-0.8544
	h	$[Asp + H]^+$	134	134.0447	134.0448	-0.7952
		$[Asp + H - H_2O]^+$	116	116.0342	116.0342	-0.3971
	i	$[Tyr + H]^+$	182	182.0809	182.0812	-1.2122
		$[Tyr + H + O]^+$	198	198.0758	198.0761	-1.4860
		$[Tyr + H - H_2CO_2]^+$	136	136.0756	136.0757	-0.8819
	j	$[Ala + H]^+$	90	90.0549	90.0550	-0.9440
	k	$[Phe + H]^+$	166	166.0860	166.0863	-1.7571
		$[Phe + H - H_2CO_2]^+$	120	120.0805	120.0808	-1.9710
	l	$[Met + H]^+$	150	150.0580	150.0583	-2.3060
		$[Met + H + O]^+$	166	166.0530	166.0532	-1.3530
Figure S3 (Q Exactive™ Orbitrap™ MS)	a	$[Asn - H]^-$	131	131.0463	131.0462	0.4170
		$[Asn - 2H - H]^-$	129	129.0309	129.0306	2.2351
		$C_3H_5O_3^-$	89	89.0244	89.0244	-0.4739
	b	$[Asp - H]^-$	132	132.0301	132.0302	-0.5130
		$[Asp - H - NH_3]^-$	115	115.0037	115.0037	-0.2766
		$C_3H_5O_3^-$	89	89.0244	89.0244	-0.4739
	c	$[Trp - H]^-$	203	203.0828	203.0826	0.7153
		$[Trp - H + O]^-$	219	219.0776	219.0775	0.2411
		$[Trp - H + 2O]^-$	235	235.0725	235.0724	0.2749
		$[Trp - H + 3O]^-$	251	251.0674	251.0673	0.3517
		$[Trp + C_3H_5O_3]^-$	293	293.1145	293.1143	0.8168
		$C_3H_5O_3^-$	89	89.0244	89.0244	-0.4739
	d	$[Ala - H]^-$	88	88.0404	88.0404	0.2570
		$[Ala - 2H - H]^-$	86	86.0250	86.0248	2.3477
		$C_3H_5O_3^-$	89	89.0244	89.0244	-0.4739
	e	$[Phe - H]^-$	164	164.0718	164.0717	0.3827
		$[Phe - 2H - H]^-$	162	162.0563	162.0561	1.5819
		$[Phe - H + O]^-$	180	180.0667	180.0666	0.2992
		$C_3H_5O_3^-$	89	89.0244	89.0244	-0.4739
	f	$[Met - H]^-$	148	148.0438	148.0438	0.3200
		$[Met - 2H - H]^-$	146	146.0282	146.0281	0.5990
		$[Met - H + O]^-$	164	164.0387	164.0387	0.2000
		$[Met + C_3H_5O_3]^-$	238	238.0757	238.0755	0.8960
		$C_3H_5O_3^-$	89	89.0244	89.0244	-0.4739
	g	$[Asn - H]^-$	131	131.0463	131.0462	0.4170
		$[Asn - 2H - H]^-$	129	129.0309	129.0306	2.2351
	h	$[Asp - H]^-$	132	132.0301	132.0302	-0.5130
		$[Asp - H - NH_3]^-$	115	115.0037	115.0037	-0.2766
	i	$[Trp - H]^-$	203	203.0828	203.0826	0.7153
		$[Trp - H + O]^-$	219	219.0776	219.0775	0.2411
		$[Trp - H + 2O]^-$	235	235.0725	235.0724	0.2749
		$[Trp - H + 3O]^-$	251	251.0674	251.0673	0.3517
		$[Trp + C_3H_5O_3]^-$	293	293.1145	293.1143	0.8168
		$C_3H_5O_3^-$	89	89.0244	89.0244	-0.4739
	j	$[Ala - H]^-$	88	88.0404	88.0404	0.2570
		$[Ala - 2H - H]^-$	86	86.0250	86.0248	2.3477
		$C_3H_5O_3^-$	89	89.0244	89.0244	-0.4739
	h	$[Phe - H]^-$	164	164.0718	164.0717	0.3827
		$[Phe - 2H - H]^-$	162	162.0563	162.0561	1.5819
		$[Phe - H + O]^-$	180	180.0667	180.0666	0.2992
		$C_3H_5O_3^-$	89	89.0244	89.0244	-0.4739
	l	$[Met - H]^-$	148	148.0438	148.0438	0.3200
		$[Met - 2H - H]^-$	146	146.0282	146.0281	0.5990
		$[Met - H + O]^-$	164	164.0387	164.0387	0.2000
		$[Met + C_3H_5O_3]^-$	238	238.0757	238.0755	0.8960

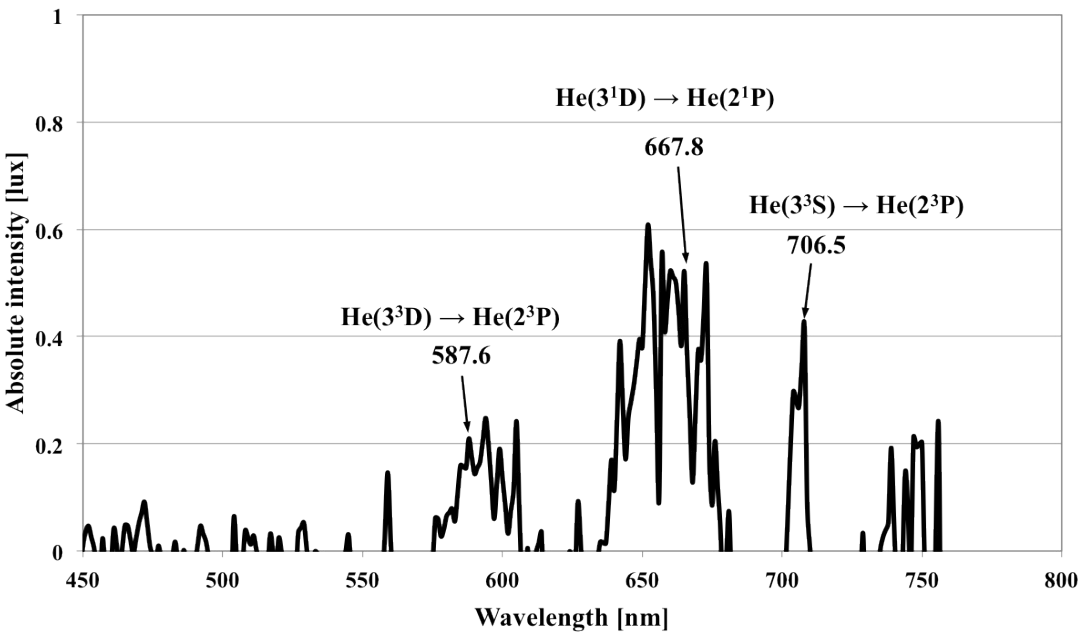

Figure S1. Visible spectrum of purple-glowing He gas flow shown in Fig. 1b.

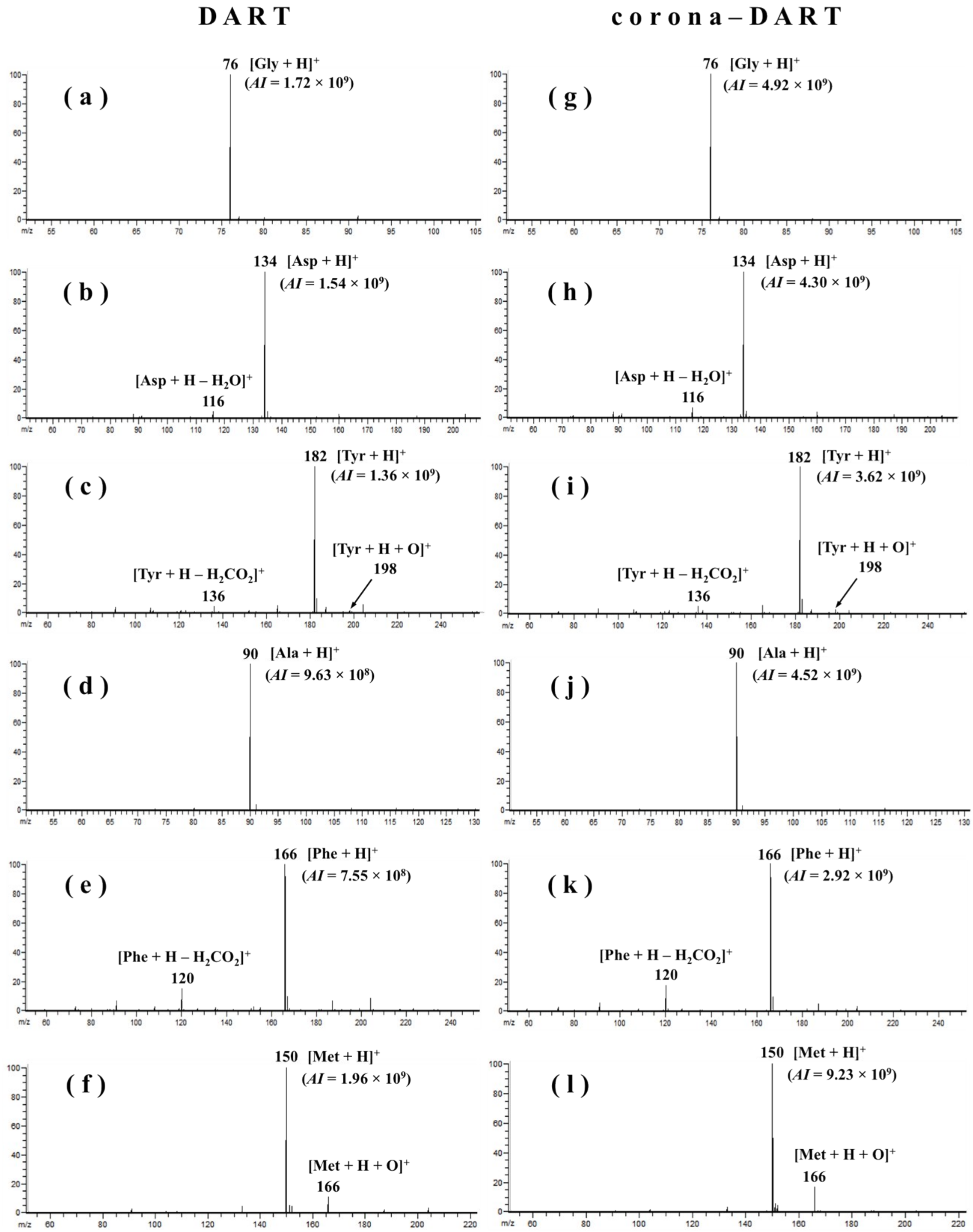

Figure S2. Positive-ion mass spectra of Gly, Asp, Tyr, Ala, Phe and Met obtained by (a – f) DART or (g – l) corona-DART ionization coupled with a Q Exactive™ Orbitrap™ mass spectrometer. *AI* represents the absolute intensity (arbitrary units) of a given ion. The exact masses of the analyte-related ions observed in each mass spectrum and the corresponding accuracy are summarized in Table S1.

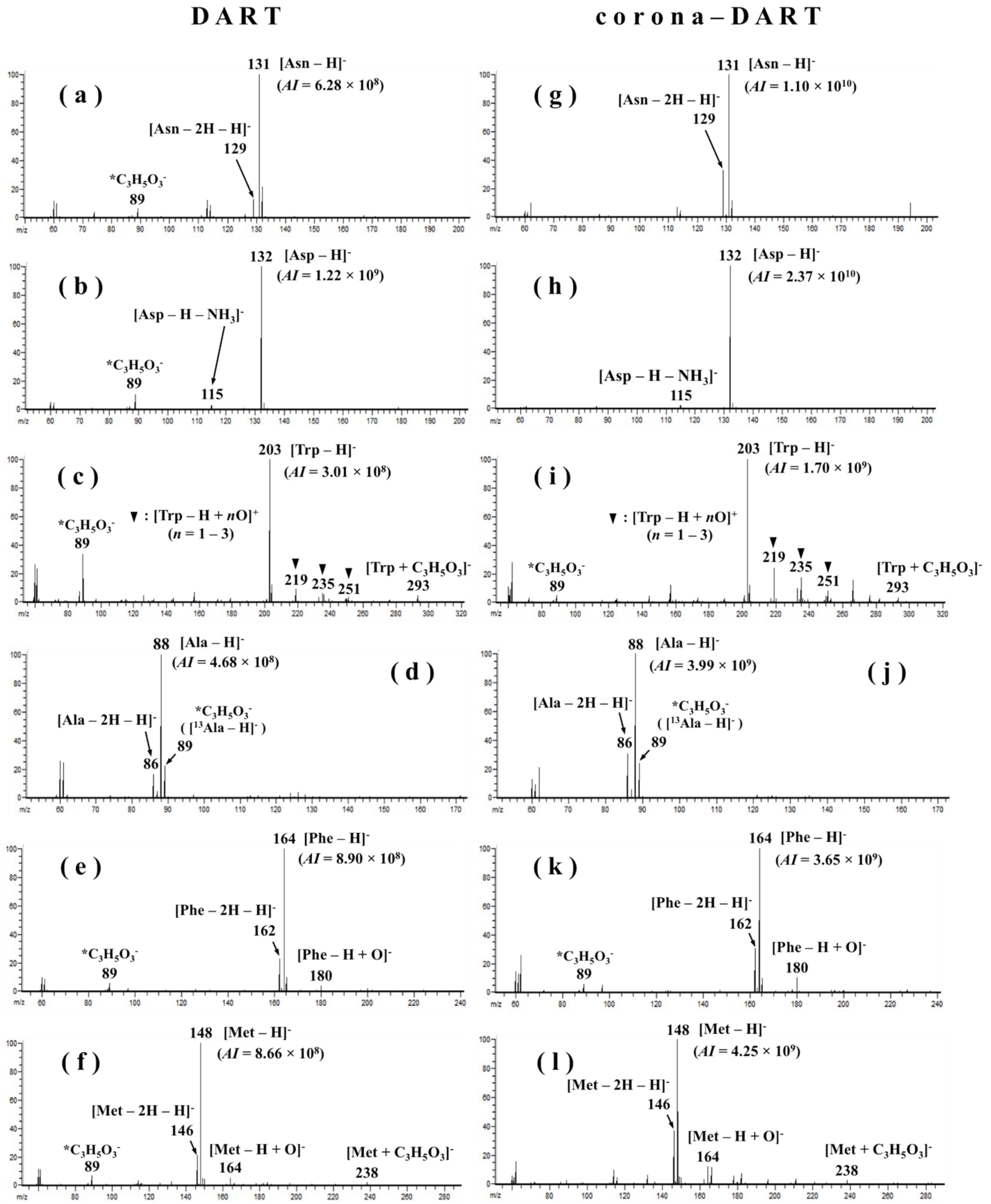

Figure S3. Negative-ion mass spectra of Asn, Asp, Trp, Ala, Phe and Met obtained by (a – f) DART or (g – l) corona-DART ionization coupled with a Q Exactive™ Orbitrap™ mass spectrometer. The ions with asterisk (*) correspond to deprotonated lactic acid as negative background ions. *AI* represents the absolute intensity (arbitrary units) of a given ion. The exact masses of the analyte-related ions observed in each mass spectrum and the corresponding accuracy are summarized in Table S1.

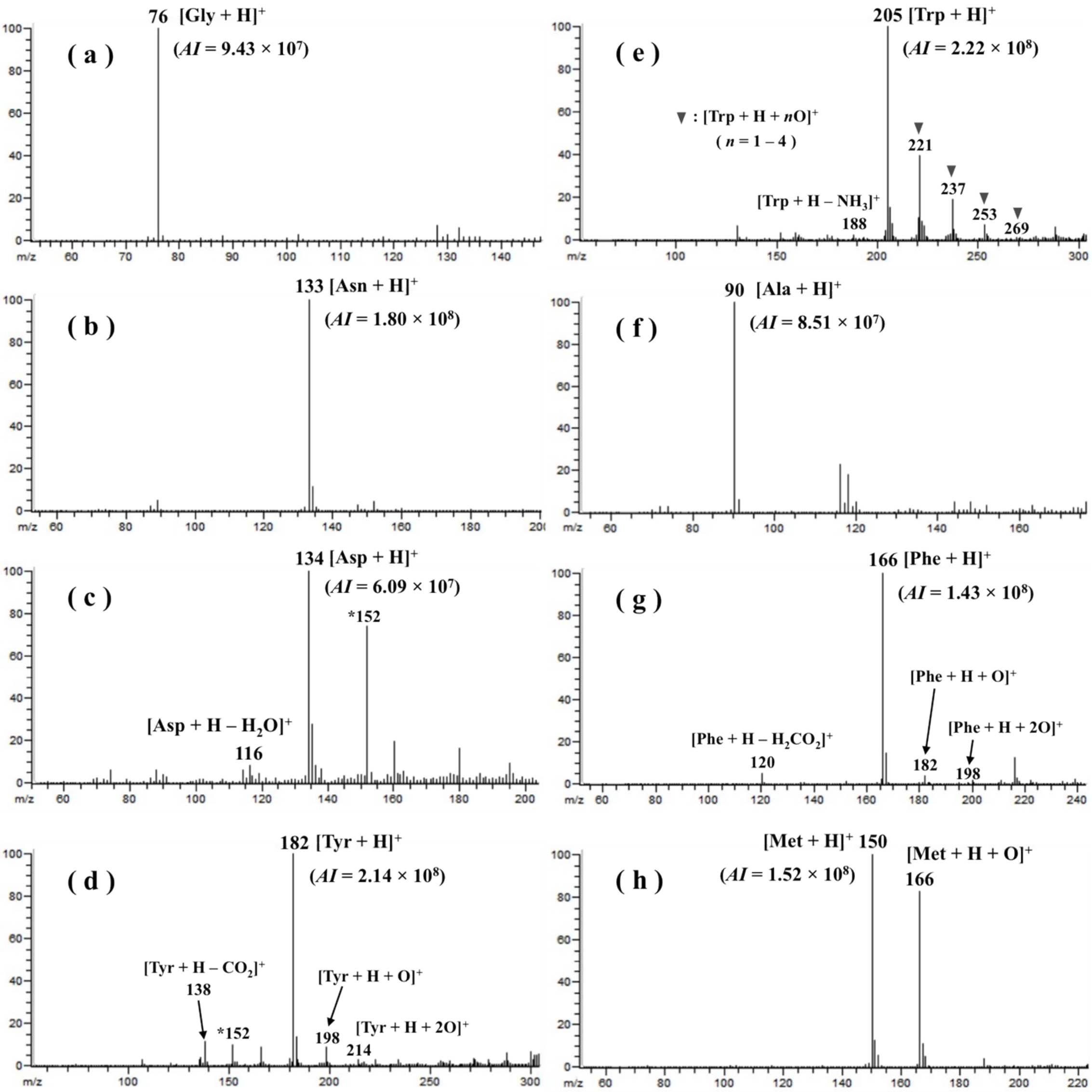

Figure S4. Positive-ion mass spectra of (a) Gly, (b) Asn, (c) Asp, (d) Tyr, (e) Trp, (f) Ala, (g) Phe and (h) Met obtained via corona-DART ionization coupled with a LCQ ion-trap mass spectrometer. The ions with asterisks (*) correspond to positive background ions. *AI* represents the absolute intensity (arbitrary units) of a given ion.

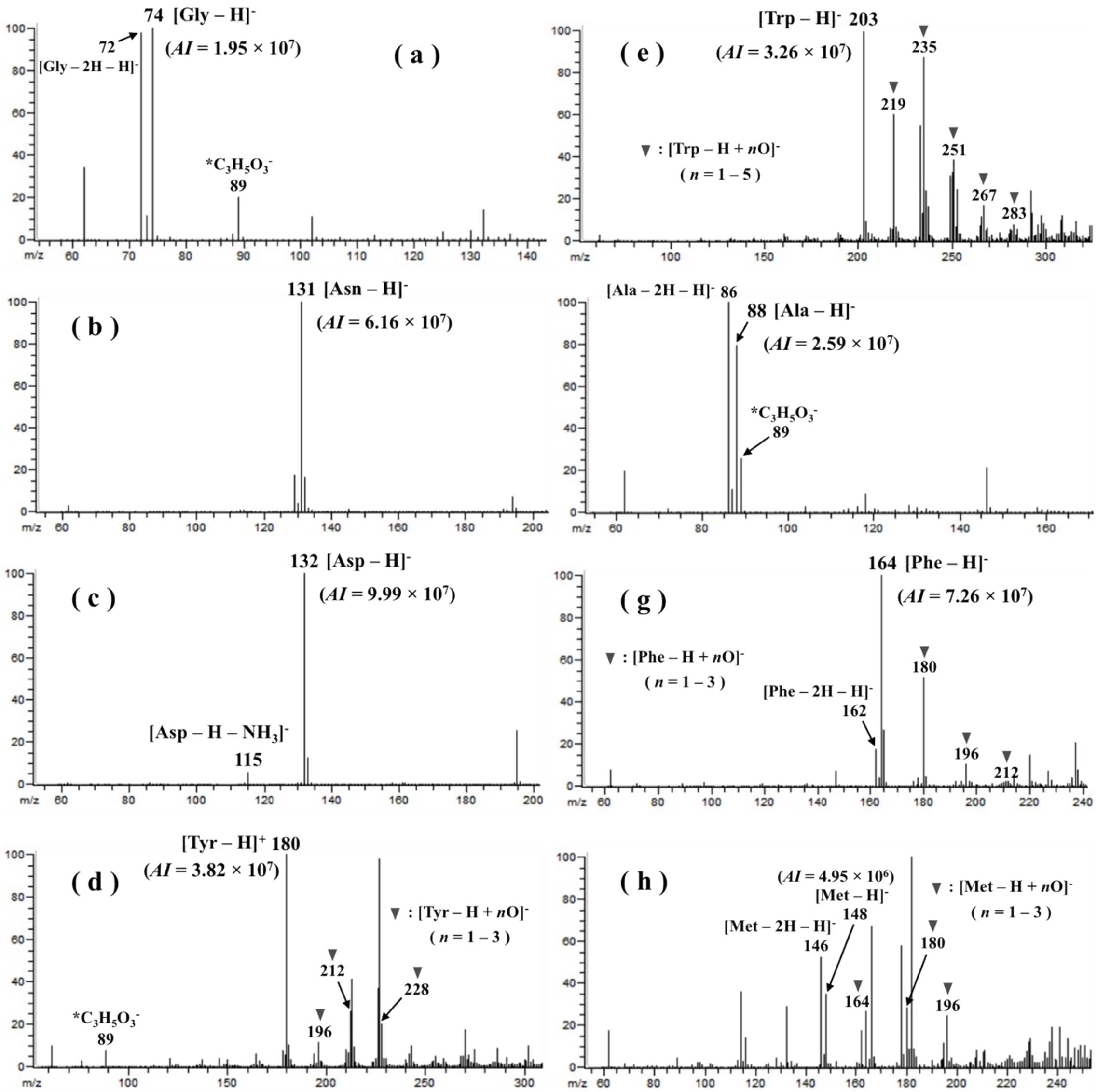

Figure S5. Negative-ion mass spectra of (a) Gly, (b) Asn, (c) Asp, (d) Tyr, (e) Trp, (f) Ala, (g) Phe and (h) Met obtained by corona-DART ionization coupled with a LCQ ion-trap mass spectrometer. The ions with asterisks (*) correspond to deprotonated lactic acid as negative background ions. *AI* represents the absolute intensity (arbitrary units) of a given ion.

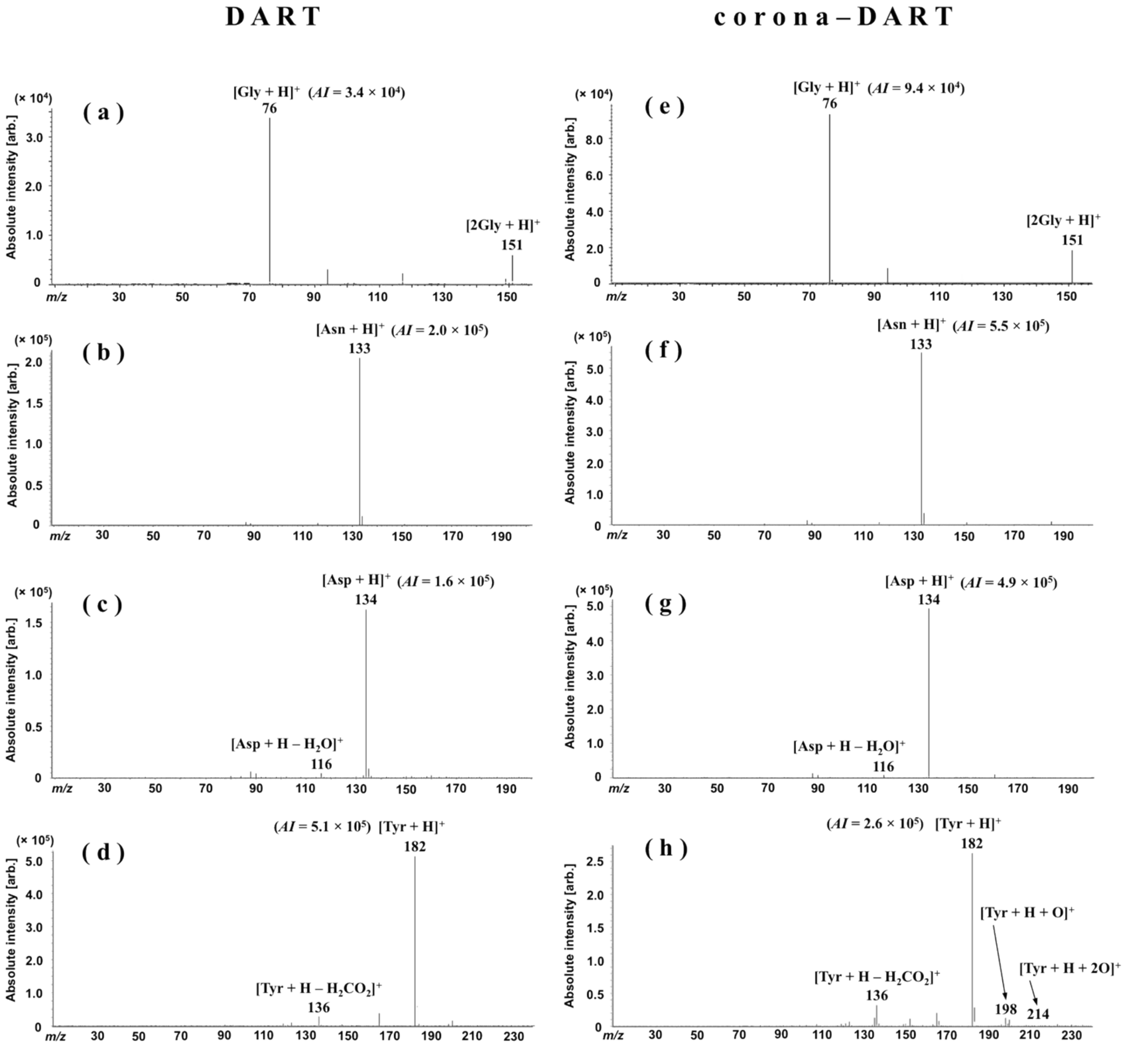

Figure S6. Positive-ion mass spectra of Gly, Asn, Asp and Tyr obtained by (a – d) DART or (e – h) corona-DART ionization coupled with a LCMS-2020 quadrupole mass spectrometer. *AI* represents the absolute intensity (arbitrary units) of a given ion.

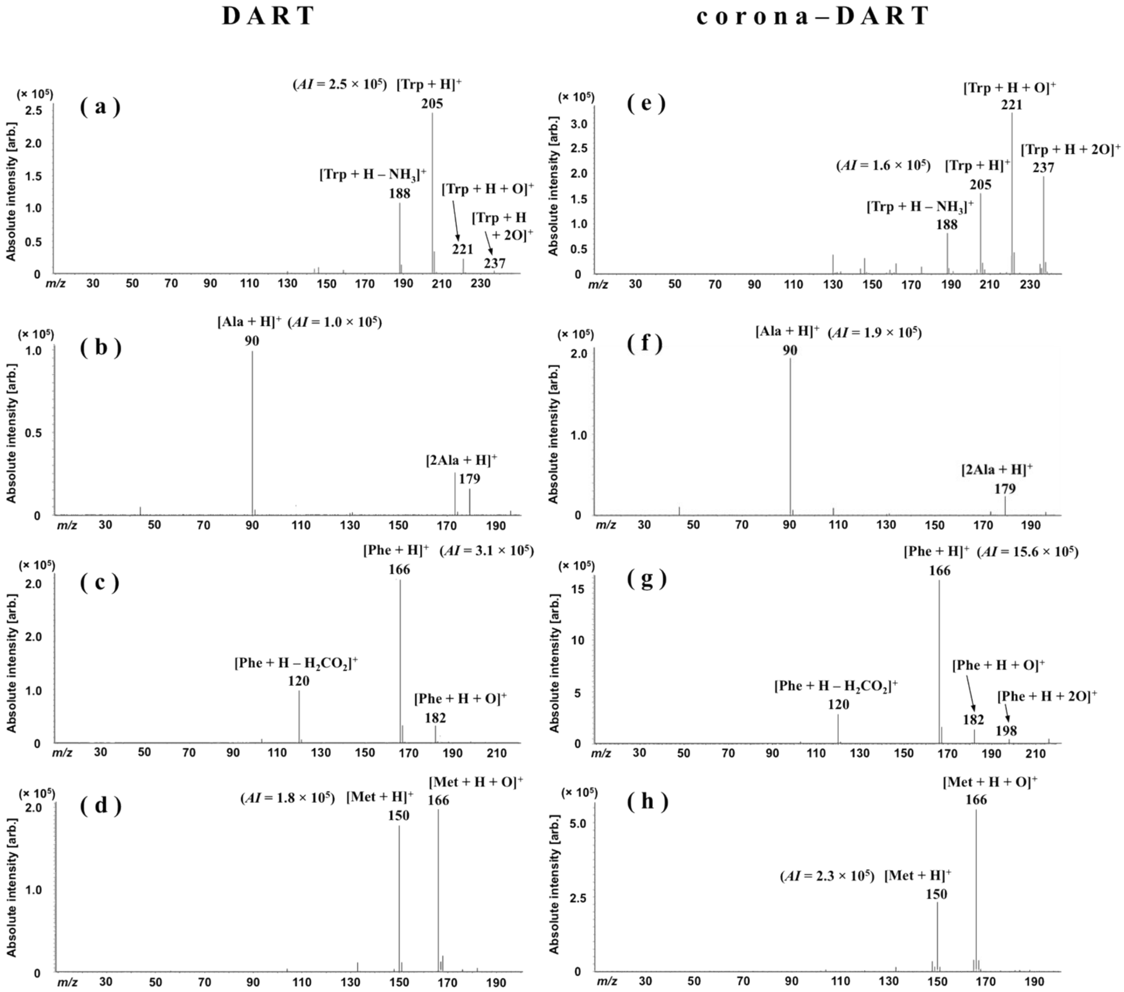

Figure S7. Positive-ion mass spectra of Trp, Ala, Phe and Met obtained by (a – d) DART or (e – h) corona-DART ionization coupled with a LCMS-2020 quadrupole mass spectrometer. *AI* represents the absolute intensity (arbitrary units) of a given ion.

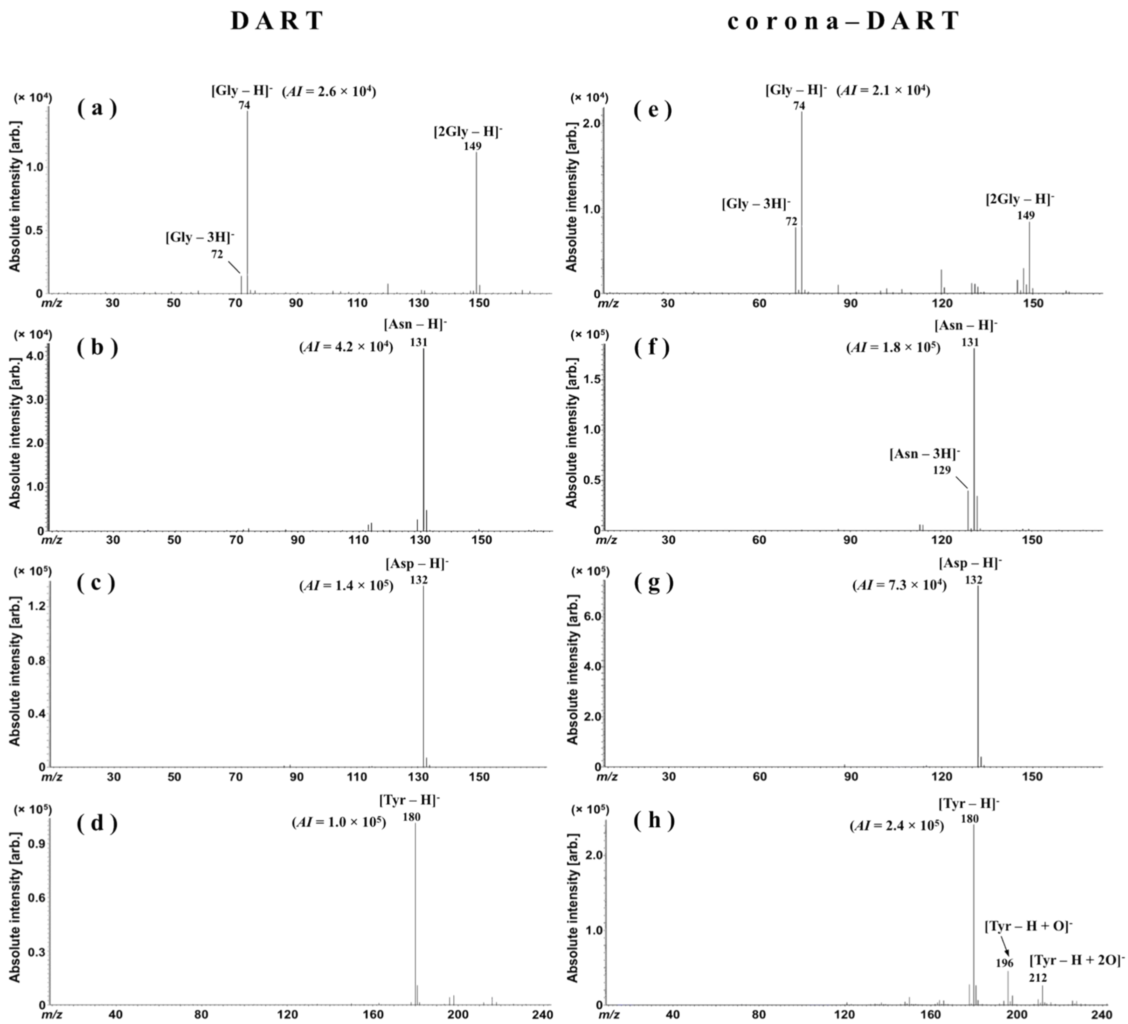

Figure S8. Negative-ion mass spectra of Gly, Asn, Asp and Tyr obtained by (a – d) DART or (e – h) corona-DART ionization coupled with a LCMS-2020 quadrupole mass spectrometer. *AI* represents the absolute intensity (arbitrary units) of a given ion.

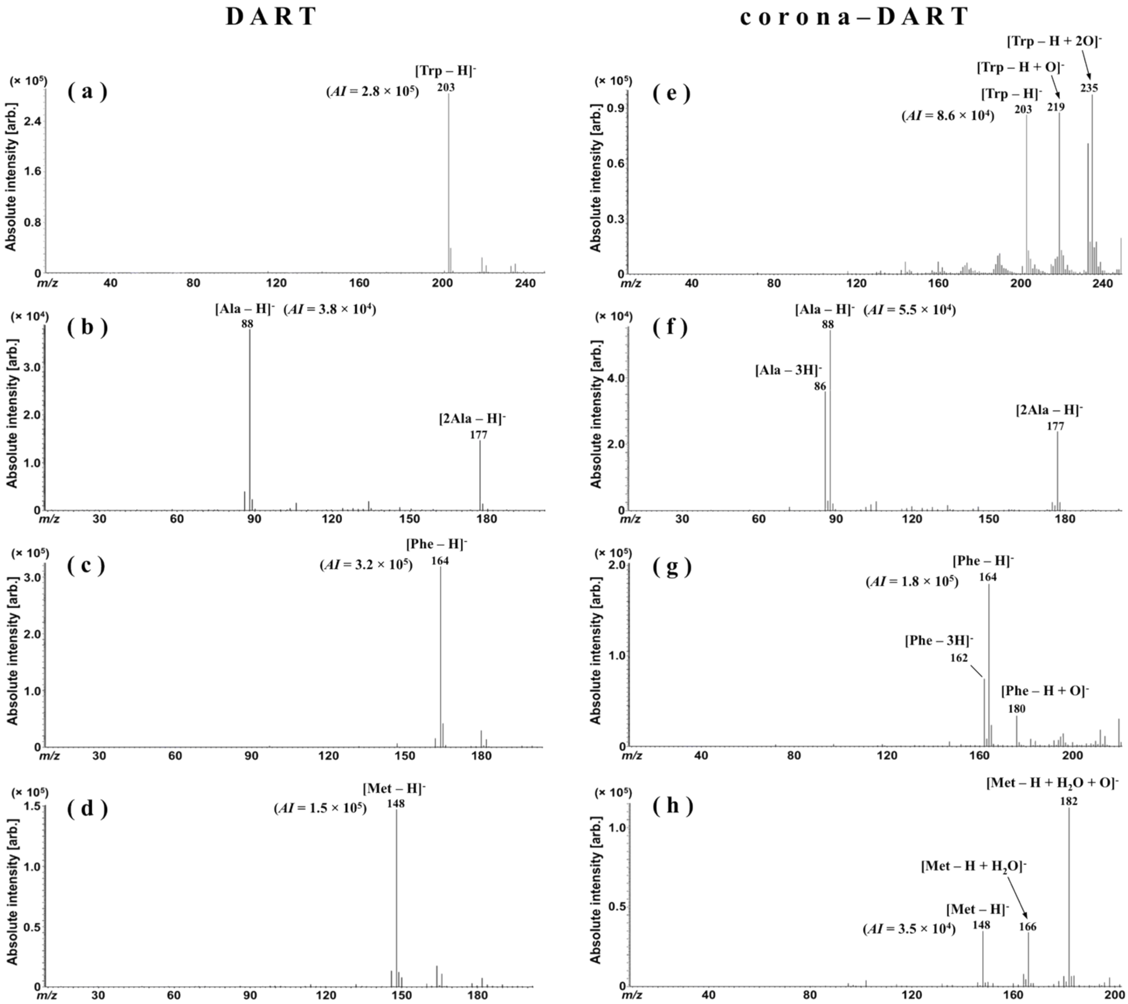

Figure S9. Negative-ion mass spectra of Trp, Ala, Phe and Met obtained by (a – d) DART or (e – h) corona-DART ionization coupled with a LCMS-2020 quadrupole mass spectrometer. *AI* represents the absolute intensity (arbitrary units) of a given ion.

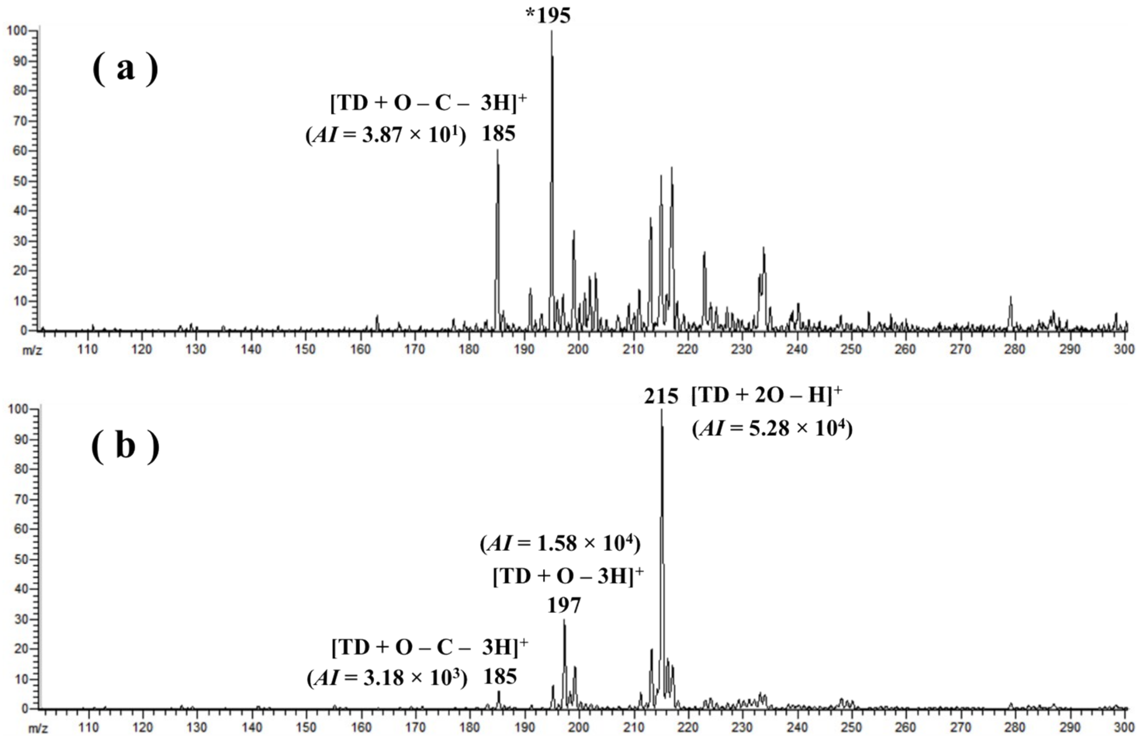

Figure S10. Positive-ion mass spectra of *n*-tridecane obtained with (a) DART and (b) corona-DART ionization coupled with a LCQ Deca XP ion-trap mass spectrometer. The ion with an asterisk (*) corresponds to the positive background ion. *AI* represents the absolute intensity (arbitrary units) of a given ion.

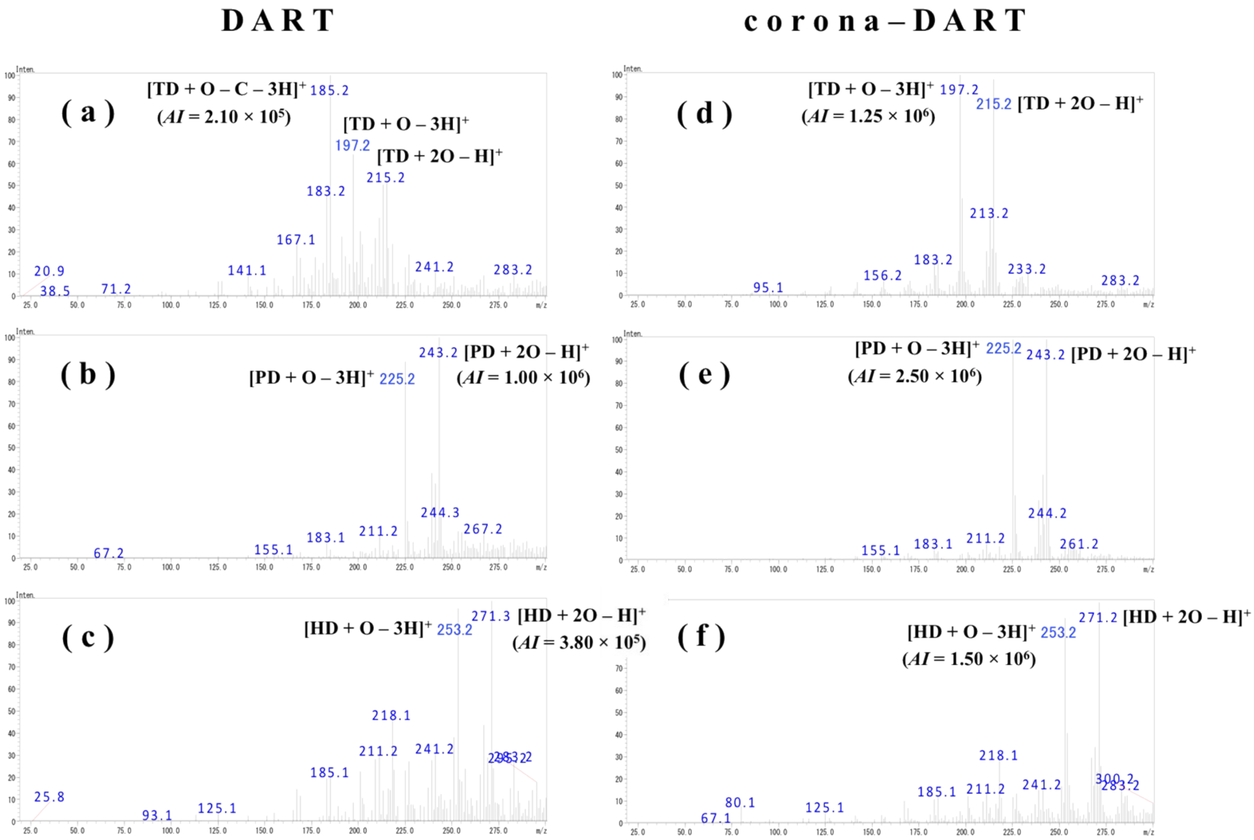

Figure S11. Positive-ion mass spectra of 3 different alkanes obtained with DART and corona-DART ionization coupled with a LCMS-2020 quadrupole mass spectrometer. The experimental conditions used (analyte, ionization method) were (a) (*n*-tridecane, DART), (b) (*n*-pentadecane, DART), (c) (*n*-heptadecane, DART), (d) (*n*-tridecane, corona-DART), (e) (*n*-pentadecane, corona-DART) and (f) (*n*-heptadecane, corona-DART). *AI* represents the absolute intensity (arbitrary units) of a given ion.